

Adsorption of individual C_{60} molecules on Si(111)

Y. Z. Li, M. Chander, J. C. Patrin, and J. H. Weaver

Department of Materials Science and Chemical Engineering, University of Minnesota, Minneapolis, Minnesota 55455

L. P. F. Chibante and R. E. Smalley

Rice Quantum Institute and Department of Chemistry and Physics, Rice University, Houston, Texas 77251

(Received 21 January 1992)

Scanning tunneling microscopy (STM) and spectroscopy studies have been conducted for individual C_{60} molecules adsorbed on Si(111)- 7×7 surfaces. C_{60} molecules appear to be immobilized following condensation at 300 K. Bias-dependent STM imaging and current-imaging tunneling spectroscopy data illustrate different C_{60} bonding configurations.

The structural and electronic properties of the fullerene molecule, C_{60} , have been studied extensively and there have been several investigations of surfaces and interfaces of these materials.¹ Experimental investigations using scanning tunneling microscopy (STM) have shown that C_{60} forms hexagonally symmetric two-dimensional islands on Au(111),² but weak surface bonding causes structural instabilities in the C_{60} islands. In contrast, translational motion of C_{60} molecules in large two-dimensional islands on GaAs(110) was not evident, and specific adsorption structures were determined.³ STM studies of C_{60} on GaAs(110) also showed monolayer films with corrugation that relieved internal strain, and ordered structures, defects, dislocations, and grain structures were observed for multilayers.³ Photoemission studies of C_{60} monolayers on metal and GaAs substrates demonstrated charge transfer and partial occupancy of levels derived from the lowest unoccupied molecular orbital (LUMO).⁴

This study focuses on individual C_{60} molecules adsorbed on Si(111)- 7×7 . STM imaging shows that the randomly distributed molecules remain isolated after deposition at 300 K. Bias-dependent imaging and current-imaging tunneling spectroscopy reveal different bonding configurations for C_{60} .

The fullerenes were formed by the contact arc method,⁵ with subsequent separation by solution with toluene. Phase-pure C_{60} was obtained by a liquid chromatography process on alumina diluted with mixtures of hexanes. The resulting fullerenes were rinsed in methanol, dried, and sublimed in the STM chamber. During C_{60} sublimation, the chamber pressure reached $\sim 8\times 10^{-10}$ Torr but quickly recovered to the base pressure in the 10^{-11} -Torr range. The Si(111) substrate was cleaned by flashing to ~ 1500 K to achieve the 7×7 reconstruction. It was held at ~ 300 K during C_{60} deposition. Electrochemically etched W tips were cleaned by electron beam bombardment prior to imaging. Length scales were calibrated with the Si(111)- 7×7 lattice and with double-layer atomic steps.

Figure 1 shows a typical area of the Si(111)- 7×7 surface after fractional-monolayer C_{60} deposition. The unoccupied electronic states were imaged using a sample bias voltage of 1.5 V and a tunneling current of 0.07 nA. Clearly evident are the 12 adatoms that define the unit

cell of Si(111)- 7×7 . Each bright feature against the 7×7 background represents a C_{60} molecule. These molecules remain isolated upon adsorption at 300 K, in contrast to migration and island formation on Au(111) and GaAs(110).^{2,3} Mapping onto the 7×7 lattice reveals approximately equal numbers on faulted and unfaulted



FIG. 1. A mosaic of STM images depicting C_{60} adsorption on Si(111)- 7×7 surface. The Si 7×7 reconstruction is represented by unit cells of twelve adatoms in the background. Each bright feature corresponds to an individual C_{60} molecule. The molecules remain isolated and randomly distributed. No enhanced sticking is observed at the double-layer atomic step shown as the overexposed region at the left or the domain boundary marked by arrows. The inset shows a curvature-enhanced high-resolution image of two C_{60} molecules indicated by an arrow in the mosaic.

halves of the unit cell. Inspection of Fig. 1 shows that there is no enhanced adsorption at the double-layer atomic step at the left-hand side or the domain boundary near the bottom (marked by arrows).

The apparent heights of the C_{60} molecules in Fig. 1 are centered around 4.5 Å. This is much less than the C_{60} cage diameter of 7.1 Å or the hard sphere diameter of 10.04 Å, and it reflects the lower density of states on the molecule than on the Si substrate at this bias. The C_{60} molecules adsorbed at the corner holes measure only ~ 2.3 Å in height, presumably because they are closer to the Si surface than at other sites. Note that the corner holes should provide the strongest bonding if C_{60} -Si bonding were strictly van der Waals in character since they are the points of closest contact, but no preferred bonding at corner holes was seen. The bright C_{60} features in Fig. 1 measure ~ 15 Å in diameter at the base. This large apparent lateral size can be attributed to the electronic convolution due to a finite-sized tip. Such effects become significant when the molecular diameter is comparable to the tunneling gap width.⁶

The energy gap between the highest occupied molecular orbital and LUMO levels of C_{60} is ~ 1.6 eV,⁴ and the molecules should be invisible to STM imaging when the bias falls within the gap. That this is true can be illustrated by the images in Figs. 2(a) and 2(b) where we show the same (190×190) -Å² area probed with sample biases of -2.0 and -0.4 V, respectively. These images were acquired simultaneously by scanning the same line twice with different biases. While molecules marked *A* through *F* are essentially invisible in Fig. 2(b), those marked *G*, *H*, and *I* show significantly reduced apparent heights and *J* and *K* remained the same. No Si adatoms can be resolved in Fig. 2(b) within areas where a C_{60} feature is visible in Fig. 2(a) but invisible in Fig. 2(b). Our explanation is that the Si adatom dangling bonds have coupled with the C_{60} molecular orbitals so that localized Si dangling bond states no longer exist within the contact region.

The bias dependencies for the C_{60} molecules of Fig. 2 indicate differences in bonding with the Si substrate and,

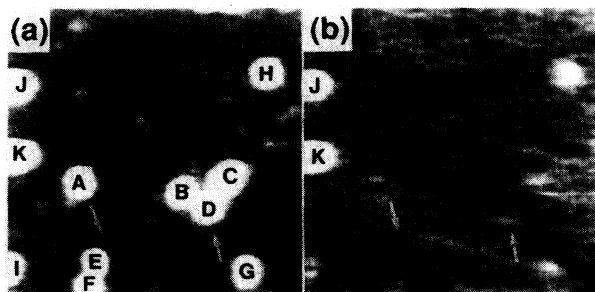


FIG. 2. Images (a) and (b) were acquired simultaneously from a (190×190) -Å² area using sample bias voltages of -2.0 and -0.4 V, respectively. The different bias dependencies of C_{60} molecules reflect their bonding configurations. Molecules *A* through *F* showed no discernible protrusion in (b) because of the lack of any density of states at this bias. Reduced protrusions were observed for *G*, *H*, and *I*, and no changes occurred for *J* and *K*. The arrows mark identical locations in two images.

hence, the electronic structure of each molecule. These differences in bonding configuration are not related to the half of the unit cell on which the molecule is located (*B* and *C* are on opposite halves of the unit cell and *D* is located between the two halves). In principle, the C_{60} pentagonal and hexagonal faces could couple differently with the Si adatom, and this could result in various bias-dependent characters. Strong substrate bonding could also restrict the rotational motion of C_{60} to ratcheting that would expose symmetry-equivalent faces. (Such ratcheting is observed for bulk C_{60} for $T < 249$ K.⁷) Previous STM studies of C_{60} on Au(111) and GaAs(110) have revealed no intramolecular structure, presumably because of nearly free rotational motion.^{2,3} Even with stronger bonding on Si(111), we found no consistent intramolecular structure at bias voltages between 3 and -3 V. The irregular height variations within single C_{60} features are shown in the inset of Fig. 1, a curvature-enhanced high-resolution image of two C_{60} molecules indicated by an arrow in the large image. These apparent intramolecular height variations had different spatial separations and directional configurations among different C_{60} molecules. Consequently, we cannot draw any definitive conclusion about their origin. The different bonding configurations for individual C_{60} molecules and the strong bias-dependent nature of the STM images made it impossible for us to correlate the observed intramolecular features to the well-known cage structure of C_{60} .

Differences in bonding configurations can be demonstrated clearly with current-imaging tunneling spectroscopy (CITS).⁸ With this technique, the surface density of states is imaged in real space with atomic resolution. Figure 3(a) shows a constant-current topographic image acquired with 0.87-V sample bias and 0.3-nA tunneling current. CITS images were acquired simultaneously for the same area with sample biases of 0.37 V for Fig. 3(b) and -0.62 V for Fig. 3(c). Images 3(b) and 3(c) resulted from taking an I - V curve at each of the 64×64 pixels scanned in 3(a) and numerically calculating the differential conductance (dI/dV) at each point. The shadow surrounding each C_{60} feature in Fig. 3(a) is an artifact related to data acquisition. The C_{60} surface density for this sample was higher than that shown in Fig. 1, and aggregates of C_{60} were formed. C_{60} molecules marked *A*, *B*, and *C* appear nearly identical in Fig. 3(a) but they show different spectroscopic characters from each other and the other molecules, as evident in their intensities in 3(b) and 3(c). Molecules that appear to be in contact also exhibit individual density-of-states characters. For example, molecules *B* and *C* show contrast in Fig. 3(b), as do the C_{60} molecules in the upper right-hand portion in the figure. This indicates that strong C_{60} -Si bonding, instead of the weak intermolecular bonding, dictates the electronic structure of an individual molecule.

With biases such as the one used for Fig. 2(b), the tip can be very close to a C_{60} molecule when scanning over it without sensing a protrusion, as reflected by some streaks in that image. This is because a typical tunneling gap is 6–10 Å wide and the C_{60} cage has a diameter of 7.1 Å. Under such bias conditions, the force between the tip and the C_{60} or the electric field exerted by close proximity can

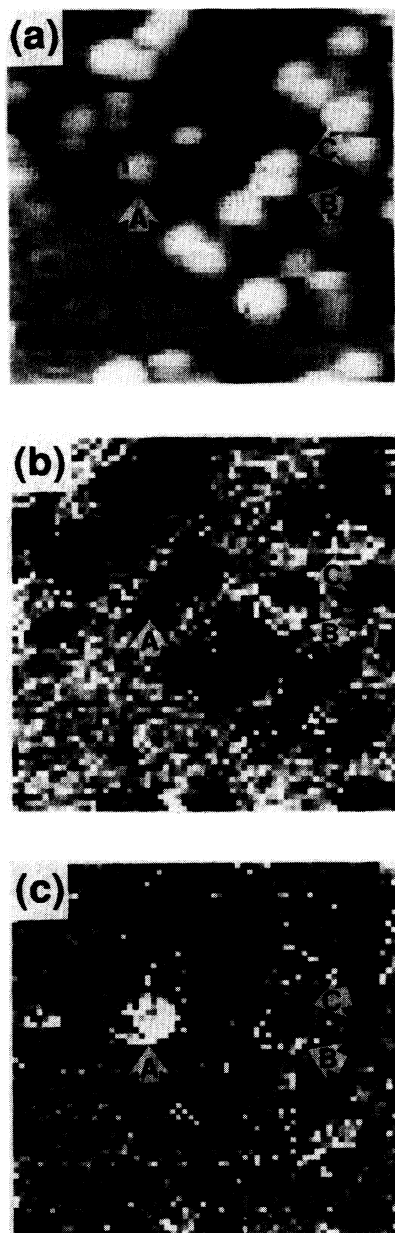


FIG. 3. (a) A constant-current topographic image, acquired with a sample bias voltage of 0.87 V, is shown along with (b), (c) differential-conductance (dI/dV) images, at 0.37- and -0.62 -V biases, respectively. Molecules *A*, *B*, and *C* exhibit distinctive density-of-state characters, as revealed by the intensity of these features in images (b) and (c), reflecting different molecular bonding configurations. The images measure $140 \times 140 \text{ \AA}^2$.

be strong enough to move the molecule. Hence, a molecule can be moved along a predefined path on the surface or it can be transferred to the tip.⁹ Figure 4 shows an example of the latter case. Molecules *A*, *B*, and *C* are evident in both images but *D* is missing in image 4(b). The process of removing *D* involved adjusting the sample bias from the imaging voltage of 2.0 to 0.6 V with the tip located at position *X*, then moving the tip to *Y* before restoring

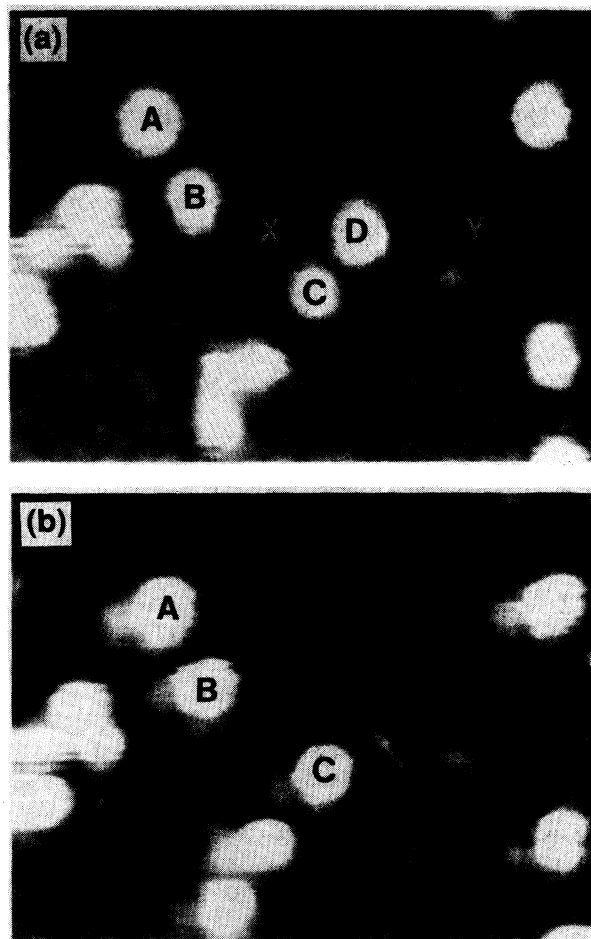


FIG. 4. (a), (b) Topographic images taken from the same $157 \times 123 \text{ \AA}^2$ surface region demonstrate the transfer of molecule *D* from the substrate to the tip. Both images were acquired with a 2.0-V bias. The tip was displaced from *X* to *Y* while closer to the molecule by reducing the bias to 0.6 V. The apparent double-tip feature in (b) is attributed to the tip shape modification after molecule *D* was picked up.

the bias voltage to 2.0 V. Comparison of Figs. 4(a) and 4(b) shows an apparent double-tip effect in 4(b), revealed by the ghost to the left of each molecule, indicating a change in the tip shape as molecule *D* was transferred to the tip. The success for such C_{60} manipulation depends on the tip used (presumably because the tip radius of curvature determines the field strength) and the particular C_{60} to be moved (because of variations in C_{60} -Si bonding).

Comparison of images 4(a) and 4(b) reveals that molecule *D* was bound to a Si adatom, indicated by an arrow in 4(b), next to a defect site. Such bonding sites may be favorable because the extra Si dangling bonds introduced by the defect could interact with the LUMO-derived π bonds of the C_{60} cage. One can compare the number density of imaged defects on surfaces with and without C_{60} to determine whether the molecules preferentially adsorb at defect sites. For a typical clean surface used in this study, the defect density was $\sim 5 \times 10^{12} \text{ cm}^{-2}$, and analysis of Fig. 1 reveals only $\sim 2 \times 10^{12} \text{ defects/cm}^{-2}$. The dif-

ference implies enhanced C_{60} adsorption at defect sites on the Si(111)- 7×7 surface. Such bonding could cause different electronic character due to variations in defect sites. Unfortunately, the large lateral extension of the C_{60} feature obscured the identification of the surface sites of adsorption. A refined technique for routinely removing C_{60} from its adsorption site may be used to gain a statistical analysis of C_{60} adsorption sites.

In summary, we have studied supported C_{60} molecules on Si(111)- 7×7 at 300 K, finding significantly different behavior than on GaAs(110) or Au(111). [Random C_{60} adsorption on Si(001)- 2×1 has also been observed. Multilayer growth at 300 K results in essentially disordered

surface structure, which is attributed to the lack of order for the first molecular monolayer.] The absence of islands indicates strong C_{60} -Si bonding and diminished molecular surface migration. Interfacial bonding most likely involves electron orbital hybridization because different bonding configurations have been observed with bias-dependent STM imaging and CITS. We have also demonstrated that a C_{60} molecule can be removed in a controlled fashion to reveal its bonding site.

This work was supported by the U.S. Office of Naval Research, the National Science Foundation, and the Robert A. Welch Foundation.

¹D. R. Huffman, *Phys. Today* **346** (11), 22 (1991), and references therein; also see *Acc. Chem. Res.* **25** (1992) for reviews of the literature.

²R. J. Wilson *et al.*, *Nature (London)* **348**, 621 (1990).

³Y. Z. Li, J. C. Patrin, M. Chander, J. H. Weaver, L. P. F. Chibante, and R. E. Smalley, *Science* **252**, 547 (1991); Y. Z. Li, M. Chander, J. C. Patrin, J. H. Weaver, L. P. F. Chibante, and R. E. Smalley, *ibid.* **253**, 429 (1991).

⁴T. R. Ohno, Y. Chen, S. E. Harvey, G. H. Kroll, J. H. Weaver, R. E. Haufler, and R. E. Smalley, *Phys. Rev. B* **44**, 13747 (1991), and references therein; P. J. Benning, D. M. Poirier, T. R. Ohno, Y. Chen, M. B. Jost, F. Stepniak, G. H. Kroll, J. H. Weaver, J. Fure, and R. E. Smalley, *ibid.* **45**, 6899 (1992).

⁵R. E. Haufler *et al.*, *J. Phys. Chem.* **94**, 8634 (1990).

⁶While imaging large surface protrusions such as C_{60} molecules,

tunneling can occur between the side of the tip and the surface feature, thus exaggerating the lateral size of the feature.

⁷P. A. Heiney, J. E. Fischer, A. R. McGhie, W. J. Romanow, A. M. Denenstein, J. P. McCauley, Jr., A. B. Smith III, and D. E. Cox, *Phys. Rev. Lett.* **66**, 2911 (1991); R. Tycko, G. Dabaghi, R. M. Fleming, R. C. Haddon, A. V. Makhija, and S. M. Zahurak, *ibid.* **67**, 1886 (1991).

⁸R. J. Hamers, R. M. Tromp, and J. E. Demuth, *Phys. Rev. Lett.* **56**, 1972 (1986); R. M. Tromp, R. J. Hamers, and J. E. Demuth, *Science* **234**, 304 (1986); R. J. Hamers, *Annu. Rev. Phys. Chem.* **40**, 531 (1989).

⁹D. M. Eigler and E. K. Schweizer, *Nature (London)* **344**, 524 (1990); D. M. Eigler, C. P. Lutz, and W. E. Rudge, *ibid.* **352**, 600 (1991); I.-W. Lyo and Ph. Avouris, *Science* **253**, 173 (1991).

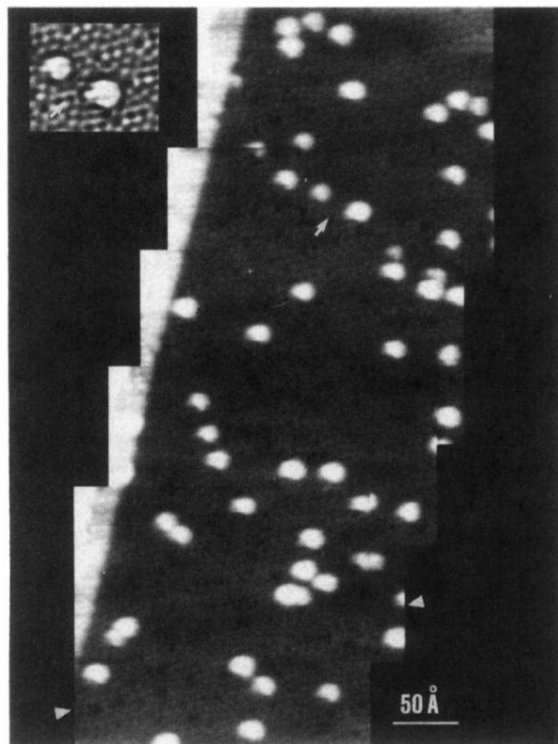


FIG. 1. A mosaic of STM images depicting C_{60} adsorption on Si(111)- 7×7 surface. The Si 7×7 reconstruction is represented by unit cells of twelve adatoms in the background. Each bright feature corresponds to an individual C_{60} molecule. The molecules remain isolated and randomly distributed. No enhanced sticking is observed at the double-layer atomic step shown as the overexposed region at the left or the domain boundary marked by arrows. The inset shows a curvature-enhanced high-resolution image of two C_{60} molecules indicated by an arrow in the mosaic.

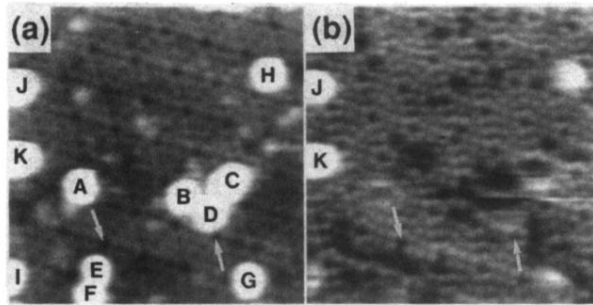


FIG. 2. Images (a) and (b) were acquired simultaneously from a $(190 \times 190)\text{-\AA}^2$ area using sample bias voltages of -2.0 and -0.4 V, respectively. The different bias dependencies of C_{60} molecules reflect their bonding configurations. Molecules *A* through *F* showed no discernible protrusion in (b) because of the lack of any density of states at this bias. Reduced protrusions were observed for *G*, *H*, and *I*, and no changes occurred for *J* and *K*. The arrows mark identical locations in two images.

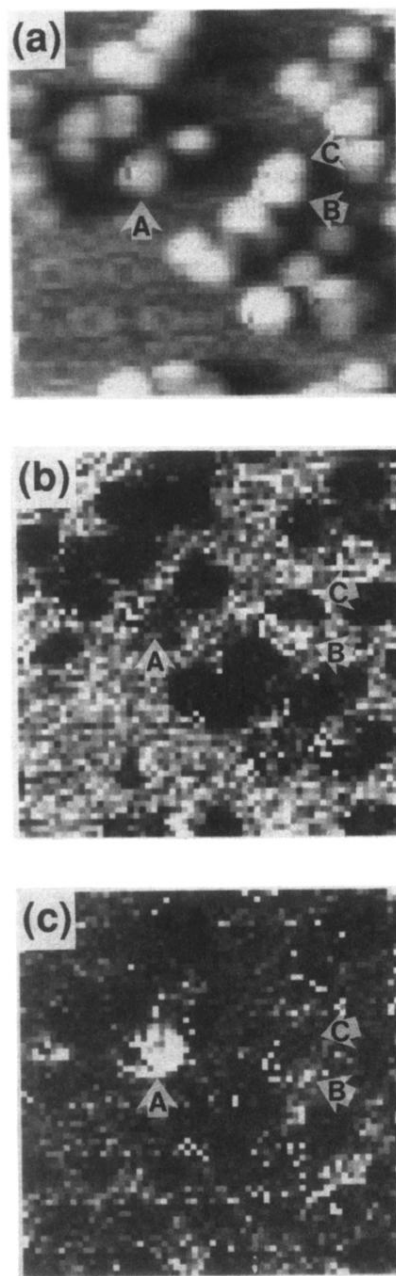


FIG. 3. (a) A constant-current topographic image, acquired with a sample bias voltage of 0.87 V, is shown along with (b),(c) differential-conductance (dI/dV) images, at 0.37- and -0.62 -V biases, respectively. Molecules *A*, *B*, and *C* exhibit distinctive density-of-state characters, as revealed by the intensity of these features in images (b) and (c), reflecting different molecular bonding configurations. The images measure $140 \times 140 \text{ \AA}^2$.

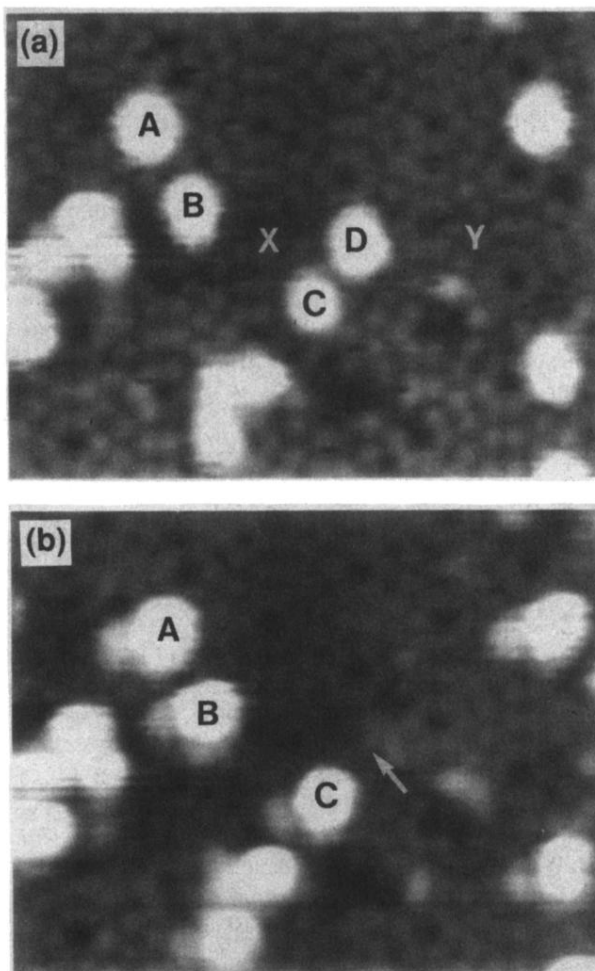


FIG. 4. (a),(b) Topographic images taken from the same $157 \times 123 \text{ \AA}^2$ surface region demonstrate the transfer of molecule *D* from the substrate to the tip. Both images were acquired with a 2.0-V bias. The tip was displaced from *X* to *Y* while closer to the molecule by reducing the bias to 0.6 V. The apparent double-tip feature in (b) is attributed to the tip shape modification after molecule *D* was picked up.